SPACE RADIATION TRANSPORT METHODS DEVELOPMENT

J.W. Wilson[1], R.K.Tripathi[1], G.D. Qualls[1], F.A. Cucinotta[2], R.E.Prael[3], J.W. Norbury[4], J.H. Heinbockel[5], and J. Tweed[5]

[1]*NASA Langley Research Center, Hampton VA 23681-2199 USA*
[2]*NASA Johnson Space Center, Houston, TX 77058 USA*
[3]*DOE Los Alamos National Laboratory, Los Alamos, NM 87545 USA*
[4]*University of Wisconsin, Milwaukee, WI 53201 USA*
[5]*Old Dominion University, Norfolk VA 23508 USA*

ABSTRACT

Improved spacecraft shield design requires early entry of radiation constraints into the design process to maximize performance and minimize costs. As a result, we have been investigating high-speed computational procedures to allow shield analysis from the preliminary design concepts to the final design. In particular, we will discuss the progress towards a full three-dimensional and computationally efficient deterministic code for which the current HZETRN evaluates the lowest order asymptotic term. HZETRN is the first deterministic solution to the Boltzmann equation allowing field mapping within the International Space Station (ISS) in tens of minutes using standard Finite Element Method (FEM) geometry common to engineering design practice enabling development of integrated multidisciplinary design optimization methods. A single ray trace in ISS FEM geometry requires 14 milliseconds and severely limits application of Monte Carlo methods to such engineering models. A potential means of improving the Monte Carlo efficiency in coupling to spacecraft geometry is given in terms of re-configurable computing and could be utilized in the final design as verification of the deterministic method optimized design.

INTRODUCTION

Following the Apollo mission, human exploration and development of space (HEDS) activity has been limited to low Earth orbit (LEO) with the advancing International Space Station (ISS) providing a first level of infrastructure for human exploration. Preparation for additional HEDS activity beyond LEO is the natural extension of the current space program. Without dispute, providing protection for astronauts and equipment from the hazards of space radiation is a critical enabling technology for future HEDS activity and one of NASA's two highest priorities (O'Keefe, 2002). Faced with a limited budget and an expanding space exploration program, the old way of doing business is inadequate and NASA requires revolutionary technologies to make advances. In none of the NASA enterprises is this more apparent than in HEDS. Radiation health risk mitigation will follow a triage involving biological, operational, and shielding countermeasures (Cucinotta et al. 2001). Environmental modeling and shielding will play important roles in this development (Wilson et al. 1997-see especially Chapters 1 and 7, also see Wilson et al. 2001a).

Early methods of space radiation shield evaluation relied largely on Monte Carlo codes (Alsmiller 1967, Lambiotte et al. 1971) and made important contributions to NASA engineering programs. Yet, slow computational procedures did not allow progress in coupling to spacecraft geometry for over 30 years (compare Alsmiller et al. 1972, Armstrong et al. 2001) and did not allow early entry of radiation constraints into the design process and off-optimum Monte Carlo solutions to shielding problems continue to plague final designs (ASAP 2000, Qualls et al.

2001, Wilson et al. 2001a). Simulations with full 3D Monte Carlo codes often use questionably simplified 1D shielding geometry models to increase computational speed in which shielding for an ISS module is approximated as a very long aluminum cylindrical shell with 20.7 g/cm^2 thickness (Badhwar et al. 2001, Armstrong and Colborn 2001) leading to an overestimate of the neutron flux and buildup of secondary charged particles within ISS since neutron leakage is underestimated (Clowdsley et al. 2002) and charged particle shielding is overestimated in these homogenized configurations (Wilson et al 1995a). Charged particle penetration estimates are improved in the 1D Monte Carlo implementation of Pinsky et al. (2001) but neutron leakage is still incorrect. A detailed examination of the influence of these various 1D simplified spacecraft geometries on the estimates of the interior environments are found to be large by Clowdsley et al. (2002). Furthermore the Monte Carlo implementations so far have been limited to a single construction material to maximize computational efficiency and optimization on multilayered optimized structures will not be possible using Monte Carlo methods because of greatly increased computational requirements.

The "3D calculations" used in current ISS Monte Carlo studies are routinely exceeded in their correctness in coupling to spacecraft geometry by HZETRN (Wilson et al. 1995a, Shinn et al. 1998, Clowdsley et al. 2001a, 2002, Qualls et al. 2001). In addition to spacecraft geometry simplifications, the astronauts in Monte Carlo calculations are approximated by a 1D sphere of tissue. Conversely, the use of a 3D Monte Carlo code within such a simplified 1D geometry for spacecraft and astronaut will often lead to erroneous underestimates of the solar particle event exposure since anisotropic shield distributions within an ISS like module have long been known to be a major factor (2 to 5) in specific astronaut organ exposure (Wilson et al. 1995a). The reason for such simplifications using Monte Carlo methods is easy to understand. To map out the interior environment of an ISS module requires at least 10^6 events within each volume about a field point. With 10^3 points for a field map, this requires 10^9 events to map the interior fields. Each particle track from boundary to exit will experience 10^3-10^4 events requiring a ray trace per event leading to 10^{12}-10^{13} ray traces for a field evaluation. In our ISS 16A configuration model in which only the HAB module is currently represented in detail (Qualls et al. 2001), 14 seconds is required to evaluate 10^3 rays with a 12 processor script on a Onyx2 parallel machine or approximately 14 msec per ray using optimized ray tracing methods (Qualls and Boykin 1997). The Monte Carlo interior field evaluation on a 12 processor Onyx2 would require 10^{10}-10^{11} seconds. It should be clear that Monte Carlo methods using ordinary central processor based computing technology will have limited usefulness in multidisciplinary design optimization.

The development of high-speed deterministic procedures allows early entry of radiation constraints into the design process without simplification of the shield geometry (Wilson and Khandelwal 1974) but Monte Carlo methods can still play a role in future final design evaluation with full geometry provided more efficient ray trace methods can be found, massively parallel machines are used, and/or a radically different approach to ray tracing can be found. We propose a radically new approach based on the use of the emerging re-configurable computing technology to *enable* Monte Carlo methods for design evaluation (but not optimization) and at the same time allow deterministic methods to map the ISS interior fields in 10's of minutes (near real-time evaluation).

At this juncture, the deterministic evaluation of multiple-elastic scattering of heavy ions has been adequately resolved with detailed laboratory testing (Schimmerling et al 1986, Shavers et al. 1990, 1993). The perplexity of straggling has been resolved (Wilson and Tai 2000, Wilson et al. 2001b, 2002). The 3D geometry in charged particle transport can be accurately approximated by added asymptotic terms (Wilson and Khandelwal 1974, Wilson 1977). The lowest order asymptotic term has been solved as a marching procedure (Wilson and Badavi 1986), a perturbation expansion (Wilson et al. 1984), a non-perturbative expansion (Wilson et al 1994a), with extensive testing in laboratory and flight experiments. Detailed investigations of the diffusive neutron component at various levels of approximation from 3D Sn methods (Singleterry and Wilson 1998) to collocation methods (Clowdsley et al. 2000) including PN methods have shown promise in approaching an efficient full 3D code but needs further development. It has been demonstrated that these methods can be used efficiently in the full 3D complexity of spacecraft design and have been flight-tested (Badhwar et al. 1995, Shinn et al. 1998, Clowdsley et al. 2002). Added treatment of the charged particle diffusive components, which will converge more rapidly than the neutral neutrons can be adequately treated using perturbation theory. A meson database needs completion (Cucinotta et al. 1998, Norbury et al. 2002) with addition of a complete E&M cascade code (Nealy et al. 2002). Further considerations of fast computational procedures and implementation issues on high performance computers for ultimate insertion into shield optimization and reliability based shield design methods are now being made (Wilson et al. 2001a, 2002, Tripathi et al. 2001, 2002).

In the present report, we will discuss the development of a fully 3D deterministic code for which past code development resulting in HZETRN is the lowest order approximation. We will also discuss the requirements for

implementing a hypercomputer algorithm to enable a potentially high-performance Monte Carlo version of LAHET useful in spacecraft design evaluation.

DETERMINISTIC CODE DEVELOPMENT

The relevant transport equations are the linear Boltzmann equations derived on the basis of conservation principles (Wilson et al. 1991a) for the flux density $\phi_j(\boldsymbol{x}, \boldsymbol{\Omega}, E)$ for particle type j as

$$\boldsymbol{\Omega}\bullet\boldsymbol{\nabla}\phi_j(\boldsymbol{x},\boldsymbol{\Omega},E)=\sum_k \int \sigma_{jk}(\boldsymbol{\Omega},\boldsymbol{\Omega}',E,E')\,\phi_k(\boldsymbol{x},\boldsymbol{\Omega}',E')\,d\boldsymbol{\Omega}'\,dE' - \sigma_j(E)\,\phi_j(\boldsymbol{x},\boldsymbol{\Omega},E) \quad (1)$$

where $\sigma_j(E)$ and $\sigma_{jk}(\boldsymbol{\Omega},\boldsymbol{\Omega}',E,E')$ are the shield media macroscopic cross sections. The $\sigma_{jk}(\boldsymbol{\Omega},\boldsymbol{\Omega}',E,E')$ represent all those processes by which type k particles moving in direction $\boldsymbol{\Omega}'$ with energy E' produce a type j particle in direction $\boldsymbol{\Omega}$ with energy E *(including decay processes)*. Note that there may be several reactions that produce a particular product, and the appropriate cross sections for equation (1) are the inclusive ones. Exclusive processes are functions of the particle fields and may be included once the particle fields are known. The total cross section $\sigma_j(E)$ with the medium for each particle type is

$$\sigma_j(E) = \sigma_{j,at}(E) + \sigma_{j,el}(E) + \sigma_{j,r}(E) \quad (2)$$

where the first term refers to collision with atomic electrons, the second term is for elastic nuclear scattering, and the third term describes nuclear reactions where we have ignored the minor nuclear inelastic processes. The corresponding differential cross section is similar. Many atomic collisions (~ 10^6) occur in a centimeter of ordinary matter, whereas ~ 10^3 nuclear coulomb elastic collisions occur per centimeter, while nuclear reactions are separated by a fraction to many centimeters depending on energy and particle type. Solution methods use the atomic collisions as a first order physical perturbation with special methods used for neutrons for which atomic cross-sections are zero.

The first order physical perturbation to the right side of equation (1) is the atomic/molecular cross sections as noted in equation (2) for which those terms in (1) are expanded about the energy moments resulting in range/energy relations including relativistic polarization effects (Shinn et al. 1993) and straggling parameters (Wilson et al. 1991, Wilson and Tai 2000, Wilson et al. 2001b, 2002). The distribution of the electrons about the ion path is critical to evaluation of biological injury (Cucinotta et al. 1995), is critical to the evaluation of shield attenuation properties (Wilson et al. 1995b), and fundamental to dosimetric evaluation of astronaut exposure risks (Shinn et al 1999). Such effects are likewise governed by equation (1). The next physical perturbation term is the coulomb scattering by the atomic nucleus and is represented by Rutherford scattering modified by screening of the nuclear charge by the orbital electrons using the Thomas-Fermi distribution for the atomic orbitals. The total nuclear coulomb cross section found by integrating over the scattering directions is related to the radiation length (Schimmerling et al.1986) and has been well validated in laboratory tests (Shavers et al. 1990, 1993). The electron production in ion collisions and the electromagnetic cascade following the neutral meson decay are described, in part, elsewhere (Cucinotta et al. 1998, Anderson et al. 2001, Nealy et al. 2002).

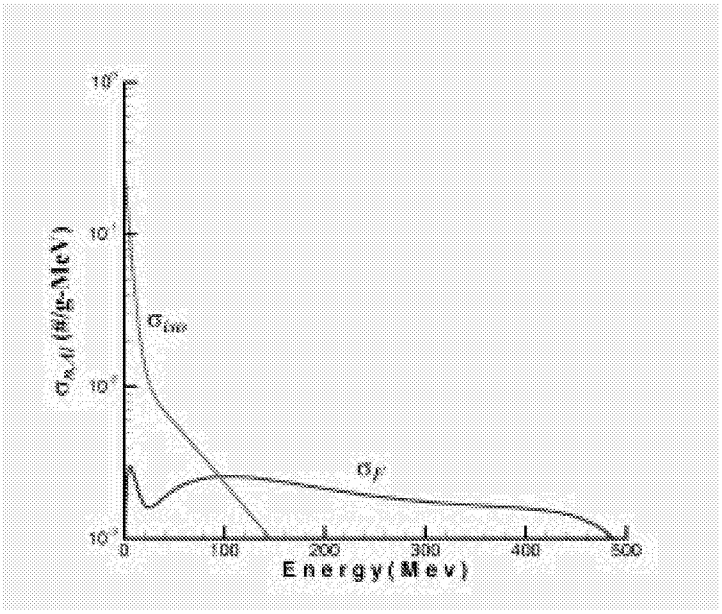

Fig. 1 Isotropic and forward neutron spectra produced by 500 MeV proton in aluminum.

The nuclear reactive differential cross sections can be written in the following form

$$\sigma_{jk,r}(\boldsymbol{\Omega},\boldsymbol{\Omega}',E,E') = \sigma_{jk,iso}(E,E') + \sigma_{jk,for}(\boldsymbol{\Omega},\boldsymbol{\Omega}',E,E') \quad (3)$$

where the first term is isotropic and associated with lower energy particles produced including target fragments and the second term is highly peaked in the forward direction and is associated mainly with direct quasi-elastic events

and projectile fragments (Wilson et al. 1988). Surprisingly even nucleon-induced reactions follow this simple form and the isotropic term extends to relatively high energies (see Fig. 1). For nucleon induced reactions, the following form has been used in versions of FLUKA (Ranft 1980) as follows

$$\sigma_{jk,r}(\boldsymbol{\Omega},\boldsymbol{\Omega}',E,E') = \nu_{jk}(E')\ \sigma_{jkr}(E')f_{jk}(E,E')\ g_R(\boldsymbol{\Omega}\bullet\boldsymbol{\Omega},E,A_T) \tag{4}$$

where the Ranft factor used in FLUKA is

$$g_R(\boldsymbol{\Omega}\bullet\boldsymbol{\Omega},E,A_T) = N_R\ exp[-\theta^2/\lambda_R]\quad \pi/2 \geq \theta \geq 0 \tag{5}$$

and constant for larger values of production angle θ and λ_R given by Ranft as

$$\lambda_R = (0.12 + 0.00036A_T/E) \tag{6}$$

although new generalized fits are being derived. This separation in phase space will be further exploited in computational procedures. The heavy ion projectile fragment cross sections are further represented by

$$\sigma_{jk,for}(\boldsymbol{\Omega},\boldsymbol{\Omega}',E,E') = \sigma_{jk,r}(E')\ N_t\ exp[-2m\sqrt{(EE')}(1-\boldsymbol{\Omega}\bullet\boldsymbol{\Omega}')/\varepsilon_{t,jk}]\ exp[-(E+\lambda_{jk}-E')^2/2\ \varepsilon_{jk}^2]/\sqrt{(2\pi\ \varepsilon_{jk}^2)} \tag{7}$$

where λ_{jk} is related to the momentum downshift, ε_{jk} is related to the longitudinal momentum width, $\varepsilon_{t,jk}$ is related to the transverse momentum width, and N_t is the transverse normalizing factor. Since the transverse width is small compared to the projectile and fragment energy the transverse function is highly peaked about the forward direction $(\boldsymbol{\Omega}\bullet\boldsymbol{\Omega}' \approx 1)$.

Atomic interactions limit the contributions of charged particles in the transport process. For example, the protons and alpha particles produced in aluminum below 100 A MeV contribute to the fluence only within a few centimeters of their collision source and the heavier ions are even more restricted (see Fig. 2). This is an important factor in that the transported secondary charged particle flux tends to be small at low energies and the role of additional nuclear reactions are likewise limited (see Fig. 3).

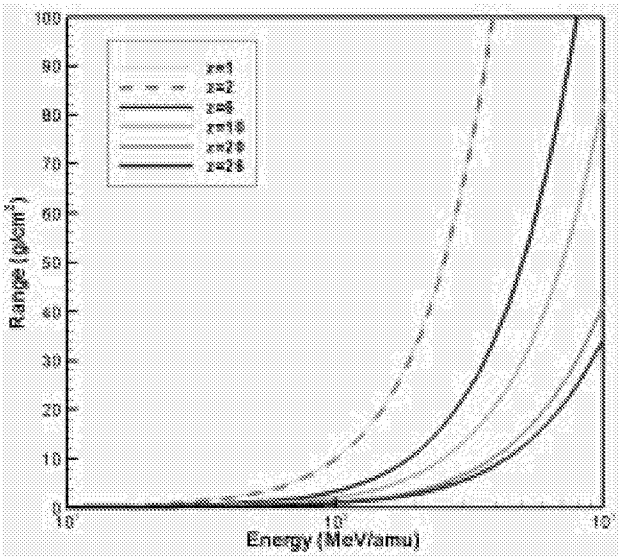

Fig. 2 Range of ions in aluminum.

We rewrite equation (1) in operator notation by defining a vector array field function as

$$\boldsymbol{\Phi} = [\phi_j(\boldsymbol{x},\ \boldsymbol{\Omega},\ E)] \tag{8}$$

the drift operator

$$\boldsymbol{D} = [\boldsymbol{\Omega}\bullet\boldsymbol{\nabla}] \tag{9}$$

and the interaction operator

$$\boldsymbol{I} = [\sum\int \sigma_{jk}(\boldsymbol{\Omega},\boldsymbol{\Omega}',E,E')\ d\boldsymbol{\Omega}'\ dE' - \sigma_j(E)] \tag{10}$$

with the understanding that $\boldsymbol{I}$ has three parts associated with atomic, elastic, and reactive processes as given in equation (2). Equation (1) is then rewritten as

$$[\boldsymbol{D} - \boldsymbol{I}_{at} - \boldsymbol{I}_{el}]\bullet\boldsymbol{\Phi} = \boldsymbol{I}_r\bullet\boldsymbol{\Phi} \tag{11}$$

where the first two physical perturbation terms are shown on the left-hand side and have been adequately resolved for ions in past research. The reaction cross section is separated by equation (3) into isotropic and forward component for which equation (11) may be written as coupled equations

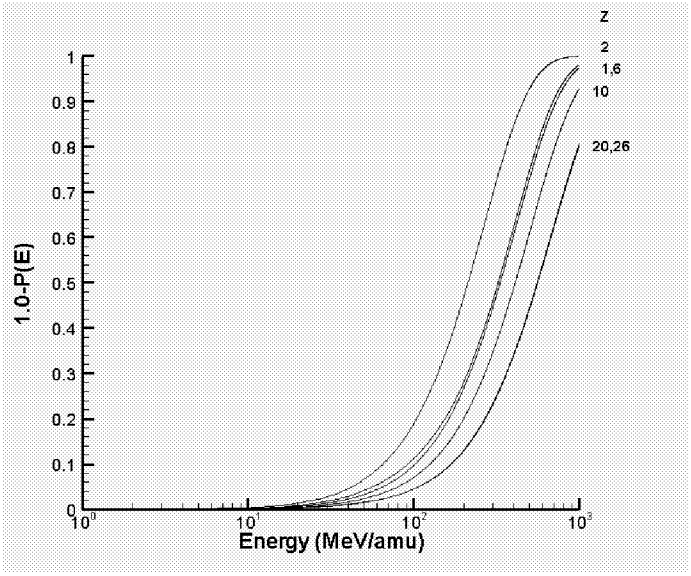

Fig. 3 Probability of nuclear reaction as a function of ion type and energy.

$$[D - I_{at} - I_{el} + \sigma_r] \bullet \Phi_{for} = \{ \int \sigma_{r,for}(\Omega,\Omega',E,E')\, d\Omega'\, dE' \} \bullet \Phi_{for} \equiv \Xi_{r,for}\, \Phi_{for} \tag{12}$$

and

$$[D - I_{at} - I_{el} + \sigma_r] \bullet \Phi_{iso} = \{ \int \sigma_r(\Omega,\Omega',E,E')\, d\Omega'\, dE' \} \bullet \Phi_{iso} + \{ \int \sigma_{r,iso}(\Omega,\Omega',E,E')\, d\Omega'\, dE' \} \bullet \Phi_{for} \equiv \Xi_r \bullet \Phi_{iso} + \Xi_{r,iso} \bullet \Phi_{f,for} \tag{13}$$

Equation (12) can be written as a Volterra equation (Wilson 1977, Wilson et al. 1991) and solved as

$$\Phi_{for} = [G + G \bullet \Xi_{r,for} \bullet G + G \bullet \Xi_{r,for} \bullet G \bullet \Xi_{r,for} \bullet G + \ldots] \bullet \Phi_B \tag{14}$$

for which the series can be either evaluated directly or proscribed as a marching procedure in either a perturbative sense as the current form of HZETRN or nonperturbative sense (future version of HZETRN) as described elsewhere (Wilson et al. 1994a).

The cross term in equation (13) gives rise to an isotropic source of light ions and neutrons of only modest energies for which Fig. 1 is typical. The high-energy portion of the isotropic spectra arises from multiple scattering effects and the Fermi motion of the struck nucleons within the nucleus. The low-energy isotropic spectra arise from nuclear decay processes. Spectral contributions to the Neuman series depend on the particle range and probability of surviving nuclear reactions that establish the functional form of the G matrix. The second term of the Neuman series is proportional to the probability of nuclear reaction that is limited by the particle range as discussed above and shown in Fig. 3. It is clear from Fig. 3 that those nuclear reactions for the charged particles below a few hundred A MeV are infrequent for which fast convergence is expected. For the moment we will neglect the straggling and multiple-elastic processes to simplify the present explanation (provide only minor corrections to space radiation exposures but important in laboratory testing) and examine the remaining reactive terms of equation (14). The corresponding Volterra equation is given by

$$\phi_j(x,\Omega,E) = \{S_j(E_\gamma)P_j(E_\gamma)\, \phi_j(\Gamma(\Omega,x),\Omega,E_\gamma) + \Sigma \int_E^{E_\gamma} dE' A_j P_j(E') \int_{E''}^{\infty} \int_{4\pi} dE'' d\Omega'\, \sigma_{jk,for}(\Omega,\Omega',E',E'') \times \phi_k(x + [R_j(E) - R_j(E')]\Omega,\Omega',E'')\} / S_j(E)P_j(E) \tag{15}$$

where Γ is the point on the boundary connected to x along $-\Omega$, $E_\gamma = R_j^{-1}[\rho - d + R_j]$, ρ is the projection of $\mathbf{x}$ onto Ω, and d is the projection of Γ onto Ω. Equation (14) results from the Neuman series solution to equation (15). In the past we have expanded the angular integral Ω' asymptotically and implemented as a marching procedure (HZETRN, Wilson and Badavi 1986), as a perturbation expansion (Wilson et al. 1984), and by non-perturbative approximation (Wilson et al. 1994a) resulting in three distinct methods to evaluate the first order asymptotic terms, all of which have had extensive experimental validation (Shavers et al. 1993, Wilson et al. 1998, Shinn et al. 1998). Independent of the method used to evaluate the lowest order term, the first correction term is found by replacing the fluence in the integrand of equation (16) by the lowest order asymptotic solution as

$$\phi_j(x,\Omega,E) = \{S_j(E_\gamma)P_j(E_\gamma)\, \phi_j(\Gamma(\Omega,x),\Omega,E) + \Sigma \int_E^{E_\gamma} dE' A_j P_j(E') \int_{E''}^{\infty} \int_{4\pi} dE'' d\Omega'\, \sigma_{jk,for}(\Omega,\Omega',E',E'') \times \phi_{k,o}(x + [R_j(E) - R_j(E')]\Omega',\Omega',E'')\} / S_j(E)P_j(E) \tag{16}$$

where $\phi_j(x,\Omega,E)$ is found as an integral over the neighborhood of rays centered on Ω using the lowest order asymptotic solution $\phi_{k,o}(x,\Omega',E'')$ along an adjacent ray directed along Ω'. Note that the boundary condition reached along $-\Omega'$ enters through the lowest order asymptotic approximation and the angular integral correction in equation (16) is determined by the homogeneity and angular dependence of the space radiation and radius of curvature of the bounding material as we have shown long ago (Wilson and Khandelwal 1974). These are the determinant factors of the magnitude of the first order asymptotic correction which is anticipated to be very small for human rated systems (large radius of curvature) in space radiation which is homogeneous and isotropic in most applications (Wilson et al. 1991, Wilson et al. 1994b).

In a region of small radius of curvature the specific flux components near the site of evaluation will be missing contributions along adjacent rays which do not compensate losses along the ray on which the solution is evaluated representing the losses due to leakage. (Note, an asymptotic treatment of such small angle dependent phenomena is the

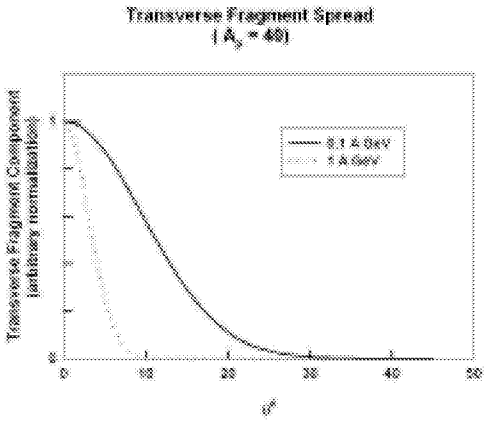

Fig. 4 Normalized transverse components for Ca fragmentation.

only useful approach circumventing large discretization errors.) This computational procedure is only a small addition to prior code development and will have little impact on computational efficiency. The angular dependence of the integral kernel of equation (16) is controlled by the forward reactive cross section $\boldsymbol{\sigma}_{jk,for}(\boldsymbol{\Omega},\boldsymbol{\Omega}',E',E'')$ with its highly peaked structure given by equations (4) or (7) depending on particle type. The angular dependence of the forward peak of fragmenting Ca ions at 100 and 1,000 A MeV is shown in Fig. 4. The low-energy ions with limited range have transverse components on the order of 10 degrees reducing to a few degrees at high energies. Note that the low energy ions have limited range and will contribute little to the transported flux (see Fig. 2) or nuclear reactions (see Fig. 3). The higher energy ions with their much longer pathlengths giving more important contributions are related to only a very small angle of acceptance (few degrees) at the boundary. The form of the kernel leads directly to a Gauss-Hermite expansion and evaluation over the angle of production. Although the neutron Neuman series for the forward components converge more slowly since their contribution to the neutron flux is not limited by atomic interactions these higher energy neutrons will be adequately evaluated by similar procedures. Higher order asymptotic terms can be evaluated with similar iteration of equation (16) if required but all indications are that the first such correction will be small for space radiation. This leaves the diffuse components of neutrons and light ions produced in the collision of the forward components and transported by equation (13) to be resolved.

The transport from the low-energy neutron and light-ion isotropic sources in equation (13) dominates the solution below about 70 A MeV (see Fig. 1). In this region light-ion transport is completely dominated by the atomic interaction terms and only a very small fraction have nuclear reactions making only minor contributions to the particle fields. This is especially true for the target fragments that can be solved in closed form (Wilson 1977, Cucinotta et al. 1991). The transport solution for the isotropic ion source terms to the lowest order perturbation is given by

$$\phi_{j,iso}{}^{o}(\boldsymbol{x},\boldsymbol{\Omega},E) = \Sigma\int_{E}^{E_\gamma} dE' A_j P_j(E') \int_{E''}^{\infty}\int_{4\pi} dE'' d\boldsymbol{\Omega}' \, \boldsymbol{\sigma}_{jkisor}(\boldsymbol{\Omega},\boldsymbol{\Omega}',E',E'') \, \phi_{k,for}(\boldsymbol{x}+[R_j(E) - R_j(E')]\boldsymbol{\Omega},\boldsymbol{\Omega}',E'')/ S_j(E)P_j(E) \quad (17)$$

and will give highly accurate solutions to equation (13) since very few of the ions will have reactions (see Fig. 3) but could be easily corrected using the HZETRN light-ion propagator applied to the diffusive source terms. Note the E' integral effectively sums the ion source terms along direction $\boldsymbol{\Omega}$ from the boundary to $\boldsymbol{x}$. Also the nuclear survival terms $P_j(E)$ are all near unity (see Fig. 3 showing $1 - P_j(E)$).

The neutrons have no charge and are undergoing, at low-energies, mainly elastic but also reactive nuclear processes. Although, equation (13) exhibits behavior similar to thermal diffusion there are strong differences between thermal and neutron diffusive processes. Thermal diffusion at ordinary temperatures has minor leakage through near boundaries since radiative processes are proportional to T^4 (in the absence of convection) leaving lateral diffusion an important process. In distinction, neutron diffusion is dominated by leakage at near forward and backward boundaries and lateral diffusion plays a minor role. Generally, low-energy neutron leakage is a dominant process within 15-20 g/cm^2 of the bounding surface in most materials. Since human rated systems have shields of large radius of curvature and small thickness to radius ratio as determined by living and working space requirements, it approximates a connected system of flat plates for which leakage at forward and backward boundaries dominates the transport. In this limit, neutron transport simplifies to a sequence of approximate 1D-transport problems with leakage at the back and forward boundaries and shows reasonable success in comparison with experimental flight data (Clowdsley et al. 2000, 2001). In the present development we will consider a convergent series of approximations to gauge accuracy of the transport procedures and allow choices of the most practical method.

The first term for diffusive neutron transport uses the lowest order perturbation similar to equation (17) given as

$$\phi_{n,iso}{}^{o}(\boldsymbol{x},\boldsymbol{\Omega},E) = \Sigma\int_{0}^{\rho-d} dx' \exp[-\sigma_n(E)\,x'] \int_{E''}^{\infty}\int_{4\pi} dE'' d\boldsymbol{\Omega}' \, \boldsymbol{\sigma}_{jkisor}(\boldsymbol{\Omega},\boldsymbol{\Omega}',E',E'') \, \phi_{k,for}(\boldsymbol{x} - x'\boldsymbol{\Omega},\boldsymbol{\Omega}',E'') \quad (18)$$

where $\rho-d$ is the distance along $-\boldsymbol{\Omega}$ from $\boldsymbol{x}$ to the boundary, x' is the distance from $\boldsymbol{x}$ to the source point along $-\boldsymbol{\Omega}$, and $\sigma_n(E)$ is the total neutron cross section. Note that equations (17) and (18) transport all particles associated with the collisions of the forward component $\boldsymbol{\Phi}_{for}$ found as solution to equation (14). The second collision term associated with the diffuse charged particle field given by equation (17) is negligible but additional source terms from the lowest-order diffuse neutron solution given by equation (18) provides a strong source of diffuse neutrons. The added transport of the neutrons is given by

$$[\boldsymbol{\Omega}\bullet\boldsymbol{\nabla} + \sigma_n(E)]\,\phi_{n,iso}{}^{1}(\boldsymbol{x},\boldsymbol{\Omega},E) = \int \boldsymbol{\sigma}_n(\boldsymbol{\Omega},\boldsymbol{\Omega}',E,E')d\boldsymbol{\Omega}'dE'\phi_{n,iso}{}^{1}(\boldsymbol{x},\boldsymbol{\Omega}',E') + \int \boldsymbol{\sigma}_{n,r}(\boldsymbol{\Omega},\boldsymbol{\Omega}',E,E')d\boldsymbol{\Omega}'dE'\phi_{n,iso}{}^{o}(\boldsymbol{x},\boldsymbol{\Omega}',E') \quad (19)$$

where $\phi_{n,iso}{}^{1}(x,\Omega,E)$ is the remaining diffuse neutron component. The source term to the far right of equation (19) have been solved in exact 3D geometry and the energy spectrum is much degraded for the source term in equation (18). Typical spectra of the sources in equations (18) and (19) are shown in Fig. 5. It is clear from the properties of the second collision source term that the diffuse spectra of neutrons from this term are highly degraded in energy and the methods developed in the nuclear engineering community for reactor applications are fully applicable and our final attention turns to solution of equation (19). Note that the software prepared for equation (19) is also applicable to nuclear reactor shielding issues with appropriate source terms.

The dominant contribution to the low-energy neutron transport in most materials is elastic scattering from the media nuclei. In our shell FEM geometry, equation (19) can be written as

$$[\mu\partial_x + \sigma_n(E)]\,\phi_{n,iso}{}^{1}(x,\mu,E) = \int \sigma_n(\Omega,\Omega',E,E')d\Omega'dE'\phi_{n,iso}{}^{1}(x,\mu',E') + \int\sigma_{n,r}(\Omega,\Omega',E,E')d\Omega'dE'\phi_{n,iso}{}^{o}(x,\Omega',E') \qquad (20)$$

where the last term on the right is the source term. The elastic scattering term in equation (20) has a unique angular contribution $\mu_0 = \Omega\bullet\Omega'$ for a given energy transfer $(E' - E)$ relating to a unique direction μ' under the integral. Standard spherical harmonic expansions of the cross sections and flux are made to develop a solution. As example, first order Legendre expansion (P1 approximation) gives the forward and backward flux as

$$\phi_{F,B} = 0.5\,\phi_0 \pm 0.75\,\phi_1 \qquad (21)$$

where ϕ_0, ϕ_1 are the Legendre coefficients of $\phi_{n,iso}{}^{1}(x,\mu,E)$ with approximate transport equation given as we have used in the past (Clowdsley et al. 2000) using multigroup and collocation methods.

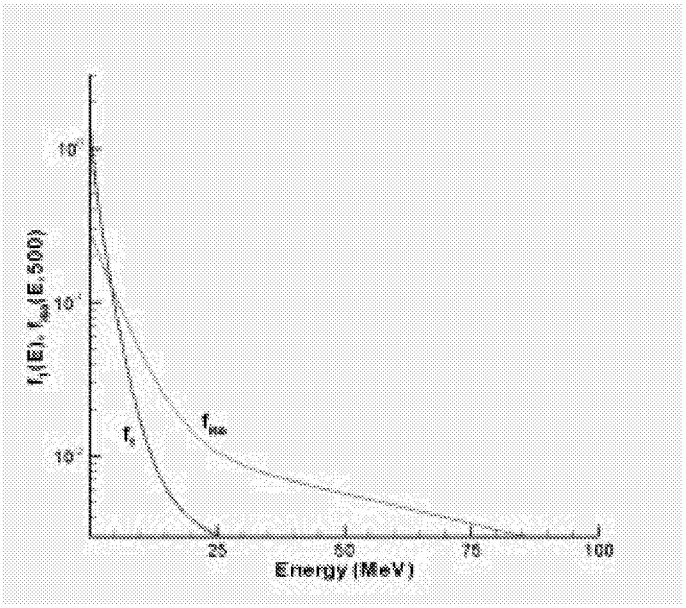

Fig. 5 Spectral dependence of diffuse isotropic neutron source term (eq. 18) and the first collision source term (eq. 19).

The multigroup transport of the diffuse neutrons in multilayered flat plate geometry with variable front and back boundaries in which the ions are treated in the lowest order asymptotic approximation is the current production HZETRN code. The first improvement would be to treat the diffuse ion components with perturbations from the neutron diffuse component giving a complete flat plate code in lowest asymptotic order with multigroup neutrons and diffuse ion components. To this we will add the first asymptotic correction. This will provide NASA with an interim HZETRN production code for engineering design process development. At each step of future improvements, the corresponding codes will be integrated into the SIREST/FACE collaborative engineering environment (Singleterry et al. 2001) with environmental models for NASA use (the current production code resides there already). To this code we will add mesons and electromagnetic cascades in the near future.

MONTE CARLO/SPACECRAFT INTERFACE DEVELOPMENT

Ray tracing procedures in combinatorial geometry is the traditional method of Monte Carlo and will not meet NASA requirements in that the models are difficult to build and don't interface with other engineering analysis packages. The ray tracing procedures in current use with deterministic codes, built on CAD geometry methods, have their origin in methods for 2D-video display. To accomplish this, the CAD models are transferred to a faceted or FEM geometry representation and mapped into a WAVEFRONT format that allows rapid ray analysis (Qualls and Boykin 1997). A FORTRAN code XRADICAL was written to quickly analyze each facet and calculate intersections. XRADICAL procedures were designed to emulate on a serial machine (or with limited parallelization) the processing similar to that found using gate arrays on high-speed video cards. Standards on CAD model development to arrive at meaningful results have been given (Qualls and Boykin 1997). Although highly optimized, the limitation of the method is the calculation and testing of many facets in typical spacecraft applications in a serial or near serial manor. For example, the 14 msec per trace using 12 parallel processors on an ORIGIN machine in the simplified ISS geometry with 62,000 facets (only the HAB module has fine detail).

The approach to resolve this computational task for Monte Carlo applications is to migrate back to gate array processing with large inherent parallel computational paths to improve the ray trace performance. To

accomplish this task, we will investigate setting up ray trace procedures on a radically new computational platform (re-configurable computer), a field programmable gate array (FPGA) with a reasonably high level language developed by STARBRIDGE. This is a fast developing technology and Langley Research Center is fortunate to have an R&D machine and close working relationship with STARBRIDGE under a Space Act Agreement. The research under this element will be to develop ray tracing procedures for relatively simple objects but more complicated than current Monte Carlo can reasonably handle as a test of the use of this technology. The success will be determined on comparisons between the serial code and the FPGA supported code. The advantage of this computer is the nearly unbound degree of parallelization giving potentially high performance similar to the high performance video card implementation. Plans will be made to scale to more realistic geometries and alternate pathways to implement such a procedure on the programmable STARBRIDGE hypercomputer. In the later stages of this work, the interface between the hypercomputer and Monte Carlo codes on a serial machine will be considered. Preliminary tests using a serial machine will be developed and the whole system optimized.

CONCLUSIONS

The NASA approach to risk mitigation involves a triage of science-based methods and relies heavily on the development of an understanding of the initial physical insult and radiobiological response mechanisms. The first line of mitigation is control of the physical insult through shielding material arrangement in the domains of human occupancy. The approaches to this problem have been discussed in terms of current technical development and limitations. The pathways to a final resolution of a high-efficiency shield code for implementation into spacecraft design processes is clear requiring only development and validation. Indeed, a reasonable software and database has already been assembled and tested in both laboratory and space flight. Additional development will be in the main only minor improvements to the existing technology and validation. The exposure of human beings to personal health risks demands the highest level of ethical awareness in order to achieve exploration without compromising the respect due to the humanity of the explorers.

REFERENCES

Alsmiller, R.G. (1967) High-energy nucleon transport and space vehicle shielding. Nucl. Sci. & Eng. 27: 158-189.

Alsmiller, R.G., Santoro, R.T., Barish, J., Claiborne, H.C. (1972) Shielding of Manned Space Vehicles Against Protons and Alpha Particles. ORNL-RSIC-35.

Anderson, B.A., Nealy, J. E., Qualls,G.D., Wilson, J.W. Kim, M.Y., Cucinotta, F.A., Atwell, W. De Angelis, G., Ware, J., and Persans, A.E. (2001) Shuttle Spacesuit (Radiation) Model Development, SAE 2001-01-2368

Armstrong, T.W., Colburn, B.L. (2001) Predictions of secondary neutrons and their importance to radiation effects inside the international space station. Radiat. Meas. 33: 229-234

ASAP, www.hq.nasa.gov/office/codeq/codeq-1.htm, 2000

Badhwar, G.D., J.U. Patel, F.A. Cucinotta, J.W. Wilson, Measurements of the secondary particle energy spectra in the space shuttle. Radiat. Meas. 24: 129-138, 1995.

Badhwar, G.D., Keith, J.E., Cleghorn, T.F. (2001) Neutron measurements onboard the space shuttle. Radiation Measurements 32: 235-241

Clowdsley, M.S., et al. (2000) A comparison of the multigroup and collocation methods for solving the low-energy neutron Boltzmann equation. Can. J. Phys. 78: 45-56

Clowdsley, M.S, Wilson, J.W., Shinn, J.L., Badavi, F.F., Heinbockel, J.H., Atwell, W. (2001a) Neutron environment calculations for low earth orbit. SAE 2001-01-2327

Clowdsley, M.S., Heinbockel, J.H., Badavi, F.F., Wilson, J.W., Shuttle induced neutron environment: Computational requirements and validation. *SAE* 2002-01-2460, 2002

Cucinotta, F. A., Wilson, J. W., Shavers, M. R., Katz, R. (1995) Effects of track structure and cell inactivation on the calculation of heavy ion mutation rates in mammalian cells. Int. J. Radiat. Biol. 69:593-600

Cucinotta, F. A.; Wilson, J. W.; and Norbury, J. W. (1998) Parameterization of Pion Energy Spectrum in Nucleon-Nucleon Collisions, NASA Technical Memorandum 1998-208722

Cucinotta, F. A.; Katz, R.; Wilson, J. W.; Townsend, L. W.; Shinn, J. L.; and Hajnal, F.(1991) Biological Effectiveness of High-Energy Protons: Target Fragmentation. Radiation Research 127:130-137.

Cucinotta, F.A., W. Schimmerling, J.W., Wilson, L.E. Peterson, G.D. Badhwar, P. Saganti, J.F. Dicello, Space radiation cancer risks and uncertainties for Mars missions. *Radiat. Res.* **156**: 682-688, 2001.

Lambiotte, J.J., Wilson, J.W., Filippas, T.A. (1971) Proper-3C: A nucleon-pion transport code. NASA TM X2158.

Nealy, J.E., B.M. Anderson, F.A. Cucinotta, J.W. Wilson, R. Katz, C.K. Chang, Transport of space environmental electrons: A simplified rapid-analysis computational procedure. NASA/TP-2002-211448, 2002.

Norbury, J.W., S.R. Blattnig, R. Norman, R.K. Tripathi, Cross-section parameterizations for pion and nucleon production from negative pion-proton collisions. NASA/TP-2002-211766, 2002.

O"Keefe, S., *Admistrator O'Keefe pitches his vision for NASA*, http://www.spaceflightnow.com/news/n0203/27okeefe/ 2002.

Pinsky, L., Carminati, F., Ferrari, A. (2001) Simulation of space Shuttle neutron measurements with FLUKA. Radiat. Meas. 33: 335-339

Qualls, G.D., Boykin, R. (1997) Space radiation shielding analysis by CAD techniques. Chpt. 17 of *Shielding Strategies for Human Space Exploration*, J.W.Wilson et al. eds, NASA CP-3360, pp. 365-382

Qualls, G.D., Wilson, J.W., Sandridge, C.A., Cucinotta, F.A., Nealy, J.E., Heinbockel, J.H., Hugger, C., Verhage, J., Anderson, B.M., Atwell, W., Zapp, N., Barber, R. (2001) International Space Station Shielding Model Development. SAE 2001-01-2370

Ranft, J. (1980) The FLUKA and KASPRO Hadronic Cascade Codes. *Computer Techniques in Radiation Transport and Dosimetry,* W. R. Nelson and T.M. Jenkins, eds, Plenum Press, pp. 339-371.

Schimmerling, W., Rapkin, M., Wong, M., Howard, J. (1986) The propogation of relativistic heavy ions in multielement beam lines. Med. Phys. 13: 217-228

Shavers, M. R., Curtis, S.B., Miller, J., Schimmerling, W. (1990) The fragmentation of 670A MeV Neon-20 as a function of depth in water. II. One-generation transport theory. Radiat. Res. 124: 117-130

Shavers, M. R.; Frankel, Kenneth; Miller, Jack; Schimmerling, Walter; Townsend, Lawrence W.; and Wilson, John W. (1993): The Fragmentation of 670 A MeV Neon-20 as a Function of Depth in Water. III. Analytic Multigeneration Transport Theory. Radiation Research, Vol. 134, No. 1, pp. 1-14.

Shinn, J. L., Farhat, H., Badavi, F. F., Wilson, J. W. (1993) Polarization Correction for Ionizaion Loss in a Galactic Cosmic Ray Transport Code (HZETRN).NASA TM 4443

Shinn, J.L.; Cucinotta, F.A.; Simonsen, L.C.; Wilson, J.W.; Badavi, F.F.; Badhwar, G.D.; Miller, J.; Zeitlin, C.; Heilbronn, L.; Tripathi, R.K.; Clowdsley, M.S.; Heinbockel, J.H.; Xapsos, M.A. (1998) "Validation of a Comprehensive Space Radiation Transport Code", *IEEE Transactions on Nuclear Science*, 45: 2711-2719

Shinn, J. L., Wilson, J. W., Singleterry, R. C., Xapsos, M. A. (1999) Implications of microdosimetry in estimation of radiation quality in space environments. Health Physics 76: 510-515

Singleterry, R. C., and J.W. Wilson, Angular Neutron Transport Investigation in the HZETRN Free-space Ion and Nucleon Transport and Shielding Computer Program, Advancements and Applications in Radiation Protection & Shielding, Nashville, TN, April 19-23, 1998

Singleterry, R.C., G.D. Qualls, J.W.Wilson, F.M. Cheatwood, J.O. Riggins, K.Y. Fan, B.D. Johns, M.S. Clowdsley, M.Y. Kim, S.L. Koontz, F.A. Cucinotta, W. Atwell, F.F. Badavi, S.A. Kayali, Collaborative Engineering Methods for Radiation Shield Design. SAE 2001-01-293, 2001.

Tripathi, R.K., Wilson, J.W., Cucinotta, F.A., Nealy, J.E., Clowdsley, M.S., Kim, M.-H. Y., Deep space mission shielding optimization. SAE 2001-01-2326, 2001.

Tripathi, R.K., Simonsen, L.C., Nealy, J.E., Troutman, P.A., Wilson, J.W., Shield optimization in simple geometry for the Gateway concept. SAE 2002-01-2332, 2002.

Wilson, J.W., Khandelwal, G.S. (1974) Proton dose approximation in convex geometry. Nucl. Tech. 23: 298-305

Wilson, J.W., Townsend, L.W., Bidasaria, H.B., Schimmerling, W., Wong, M. Howard, J. (1984) 20-Ne depth-dose relations in water. Health Phys. 46: 1101-1111

Wilson, J. W. and Badavi, F. F.: Methods of Galactic Heavy Ion Transport. Radia. Res. 108, 1986, p. 231

Wilson, J.W. (1977) Analysis of the theory of high-energy ion transport. NASA TN D-8381

Wilson, J.W. S. Y. Chun, W. W. Buck, and L. W. Townsend: High Energy Nucleon Data Bases. Health Physics, Vol. 55, November 1988, pp. 817-819

Wilson, J. W., Townsend, L. W., Schimmerling, W., Khandelwal, G. S., Khan, F., Nealy, J. E., Cucinotta, F. A., Simonsen, L. C., Shinn, J. L., Norbury, J. W. (1991) Transport Methods and Interactions for Space Radiations. NASA RP-1257

Wilson, J. W.; Shavers, M. R.; Badavi, F. F.; Miller, J.; Shinn, J. L.; and Costen, R. C. (1994a) Nonperturbative Methods in HZE Propagazition. Radiat. Res. 140: 241-244

Wilson, J. W.; Townsend, L. W.; Shinn, J. L.; Badavi, F. F.; and Lamkin, S. L.: Galactic Cosmic Ray Transport Methods: Past, Present, and Future. Adv. Space Res. 14:. (10) 841 - (10) 852, 1994.b

Wilson, J.W., Nealy, J.E., Wood, J.S., Qualls, G.D., Atwell, W., Shinn, J.L., Simonsen, L.C. (1995a) Variations in astronaut radiation exposure due to anisotropic shield distribution. Health Phys. 69: 34-45

Wilson, J. W.; Kim, M.; Schimmerling, W.; Badavi, F. F.; Thibeault, S. A.; Cucinotta, F. A.; Shinn, J. L.; and Kiefer, R.(1995b) Issues in Space Radiation Protection.: Galactic Cosmic Rays. Health Phys. 68:50-58

Wilson, J. W., Cucinotta, F. A., Tai, H., Shinn, J. L., Chun, S. Y., Tripathi, R.K., Sihver, L. (1998) Transport of light ions in matter. Adv. Space Res. 21(12): 1763-1771

Wilson, J. W., Tai, H. (2000) Range and energy straggling in ion beam transport. NASA/TP-2000-209864.

Wilson, J.W., Shinn, J.L., Tripathi, R.K., Singleterry, R.C., Clowdsley, M.S., Thibeault, S.A., Cheatwood, F.M., Schimmerling, W., Cucinotta, F.A., Badhwar, G.D., Noor, A.K., Kim, M.Y., Badavi, F.F., Heinbockel, J.H., Miller, J., Zeitlin, C.E., Heilbronn, L (2001a) Issues in deep space radiation protection. Acta Astronautica 49:289-312

Wilson, J.W., Tweed, J., Zeitlin, C.E., Kim, M.Y., Anderson, B.M., Cucinotta, F.A., Ware, J., Persans, A.E. (2001b) Shuttle Spacesuit: Fabric/LCVG model validation. SAE 2001-01-2372.

Wilson, J.W., Tweed, J., Tai, H., and Tripathi, R.K. (2002) A simple model for straggling evaluation. Nucl Inst & Methods B 194: 389-392.

Wilson, J.W., Korte, J.J., Heinbockel, J.H., Clowdsley, M.S., Badavi, F.F., Troung, A., Ionizing Radiation: Multifunctionality and MDO Processes. SAE 2002-01-2334, 2002.